

---

# Magnetic Resonance Imaging of Cardiac Tumors: Part 2, Malignant Tumors and Tumor-Like Conditions

Kiran Randhawa, MBBS, MRCS, Arul Ganeshan, MRCP, FRCR, and  
Edward T.D. Hoey, MRCP, FRCR

Cardiovascular magnetic resonance imaging (CMRI) is the reference noninvasive imaging technique for assessment and characterization of a suspected cardiac or juxta-cardiac mass. The multiplanar assessment of anatomy, tissue composition, and functional impact afforded by CMRI allows for early differentiation between a nonneoplastic mass and a tumor mass, be it benign or malignant. Malignant cardiac tumors have a poor prognosis; however, early detection and characterization confer some survival advantage, enabling early instigation of chemotherapy and/or consideration of a surgical debulking procedure. Cardiac metastases are far more common than primary tumors and are an important consideration in patients with disseminated disease. Angiosarcoma accounts for the majority of primary malignant lesions. Less common primary malignant cardiac tumors include sarcomas with myofibroblastic differentiation, lymphoma, rhabdomyosarcoma, pericardial mesothelioma, and pericardial synovial sarcoma. A number of benign masses and normal anatomical variants can cause confusion to the inexperienced observer and must be recognized to avoid unnecessary intervention. These include intracardiac thrombus, bronchogenic and pericardial cysts, and anatomical structures, such as the Crista terminalis and moderator band.

## Introduction

Cardiovascular magnetic resonance imaging (CMRI) is established as a valuable tool in the assessment of

primary and secondary cardiac malignancy. CMRI allows accurate confirmation of the presence of a space-occupying lesion, localization and assessment of the extent of involvement, evaluation of the functional impact of the lesion, as well as tissue characterization. Such information is important not only for diagnosis but also in determination of prognosis and in planning of therapy, including surgical resection.<sup>1</sup> As such, CMRI has rapidly evolved as the reference standard technique for assessment of a suspected cardiac mass.<sup>2</sup> We present a 2-part review concerning the use of CMRI in cardiac tumor assessment, focusing on tumors that most often present in adulthood. Part 1 of the review focuses on specific CMRI techniques, protocol design, and appearances of primary benign tumors. This article, part 2, covers primary and secondary cardiac malignancy and also reviews the CMRI appearances of various “tumor-like” conditions.

Primary malignant tumors of the heart are predominantly sarcomatous in nature. Malignant tumors that metastasize to the heart are 40-50 times more frequent than primary tumors.<sup>3</sup> Clinical manifestations are diverse and nonspecific and dependent on tumor size and location. Some may remain clinically silent while others can present with symptoms relating to intracardiac obstruction, arrhythmias, and/or systemic embolization.

## Malignant Primary Tumors

Malignant primary cardiac tumors can be broadly divided into sarcomas, lymphomas, and primary pericardial malignancy. Some malignant tumors may be cured by surgical resection if discovered early but, in general, their prognosis is dismal with median survival rates of 9.6-16.5 months.<sup>4</sup> Most centers advocate surgical resection when there is a likelihood of complete removal or a debulking procedure with adjuvant

From the Department of Cardiovascular and Interventional Radiology, Heart of England NHS Foundation Trust, Birmingham, West Midlands, B9 5SS, UK.

Reprint requests: Edward T.D. Hoey, MRCP, FRCR, Department of Cardiovascular and Interventional Radiology, Heart of England NHS Foundation Trust, Birmingham, West Midlands, B9 5SS, UK. E-mail: edwardhoey1@gmail.com.

Curr Probl Diagn Radiol 2011;40:169-179.

© 2011 Mosby, Inc. All rights reserved.

0363-0188/\$36.00 + 0

doi:10.1067/j.cpradiol.2010.07.002

chemotherapy if patients are severely symptomatic.<sup>5</sup> Unlike many other solid organ tumors, integrated positron-emission tomography (PET)/computed tomography (CT) imaging has not established itself in their routine evaluation, which is probably due to their low frequency. There are, however, reports of incidentally detected cardiac neoplasia on PET/CT, particularly metastatic involvement.<sup>6</sup> In suspected aggressive cardiac malignancy, it may be prudent to consider supplementary evaluation with PET/CT, particularly for detecting occult distant disease.<sup>7</sup>

Imaging findings suggestive of a malignant cardiac tumor include a right atrial location, involvement of more than 1 cardiac chamber, size >5 cm, a hemorrhagic pericardial effusion, a broad base of attachment, extension into the mediastinum or great vessels, and a “moderate,” “strong,” or heterogeneous delayed enhancement pattern. It should be noted that no single imaging feature is both highly sensitive and specific for making a diagnosis of a malignant cardiac tumor.<sup>1,8</sup>

## Sarcomas

Sarcomas account for the majority of primary malignant cardiac tumors and are the second commonest primary tumor after myxoma (Table 1).<sup>9</sup> Histologically, they are classified into 3 main subgroups: angiosarcoma, sarcoma with myofibroblastic differentiation, and rhabdomyosarcoma.

### Angiosarcoma

Angiosarcoma is the commonest malignant cardiac neoplasm. It is a highly aggressive lesion composed of irregularly shaped vascular channels lined by anaplastic epithelial cells with sizeable areas of necrosis and hemorrhage.<sup>10</sup> Peak incidence is in the fourth decade and there is a strong male predominance. Seventy-five percent have a right atrial origin and they typically fill this chamber with extensive infiltration into adjacent structures, including pericardium, vena cavae, tricuspid valve, right coronary artery, and right ventricular free wall.<sup>11</sup> The remaining 25% show origin from the other cardiac chambers or pericardium. Clinical presentation is usually at an advanced stage with symptoms of right heart failure and/or cardiac tamponade. Metastases are present in 66%-89% of cases at time of diagnosis, most frequently to the lungs, liver, bones, lymph nodes, and brain.<sup>12</sup> Prognosis is dire with few patients surviving beyond 12 months. Complete surgical resection offers the best long-term outcome but is

**TABLE 1.** Approximate frequency of both benign and malignant primary cardiac tumors

	Percentage
<b>Benign</b>	
Myxoma	50
Fibroelastoma	15
Lipoma	5
Fibroma	4
Hemangioma	1
Cystic tumor of atrioventricular nodal region	<1
Paraganglioma	<1
Other	<1
Total	75
<b>Malignant</b>	
Angiosarcoma	10
Sarcomas with myofibroblastic differentiation	
Undifferentiated pleomorphic sarcoma	5
Osteosarcoma	1
Leiomyosarcoma	<1
Fibrosarcoma	<1
Liposarcoma	<1
Myofibroblastic tumor	<1
Rhabdomyosarcoma	2
Primary lymphoma	2
Pericardial tumors	
Mesothelioma	2
Synovial sarcoma	<1
Total	25

often contraindicated because of anatomical considerations. Neoadjuvant chemotherapy in combination with surgical debulking, and followed by adjuvant chemotherapy to destroy any remaining tumor cells, may confer some survival advantage.<sup>13</sup>

### CMRI Features

CMRI demonstrates a large infiltrating broad based mass with obliteration of surrounding tissue planes. Signal intensity is heterogeneous but predominantly isointense to myocardium on T1-weighted and hyperintense on T2-weighted images, reflecting areas of tumor tissue, necrosis, and methemoglobin (Fig 1).<sup>14</sup> On steady-state free precession images, angiosarcoma is predominantly hyperintense relative to myocardium, with areas of high- and low-signal intensity corresponding to hemorrhage and necrosis, respectively. Intralesional flow voids may be seen due to the frequently large vascular channels.<sup>14</sup> Enhancement is usually avid and a “sunray” appearance has been described.<sup>15</sup>

### Sarcomas With Myofibroblastic Differentiation

These tumors represent a diverse group of neoplasms that may contain heterologous elements, such

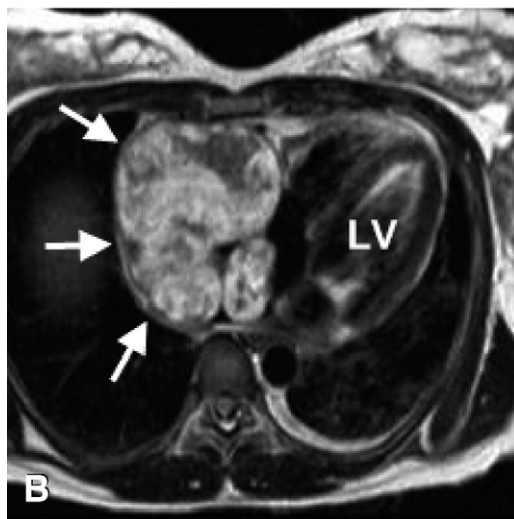
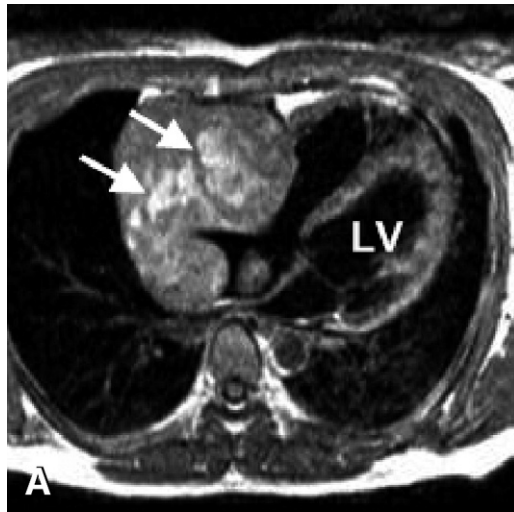


**FIG 1.** Angiosarcoma of the right atrium in a 25-year-old woman with dyspnea and chest pain. (A) Axial T1-weighted black-blood image showing a large infiltrative mass centered on the right atrial free wall. It contains central foci of high signal consistent with areas of hemorrhage (arrows). (B) Axial T2-weighted black-blood image showing the mass to be of heterogeneous high signal intensity in keeping with increased free water content (arrows). LV, left ventricle.

as bone. They predominate in adulthood, typically manifesting in the fourth or fifth decade<sup>2</sup> and are subclassified as undifferentiated sarcoma, leiomyosarcoma, fibrosarcoma, liposarcoma, and osteosarcoma. Origin is most often from the posterior wall of the left atrial wall and they typically exhibit slow infiltrative growth patterns with most patients dying of local effects rather than disseminated malignancy.<sup>5</sup> Survival depends on aggressive surgical resection but complete clearance is rarely possible, although adjuvant chemotherapy may confer some survival advantage.<sup>2</sup>

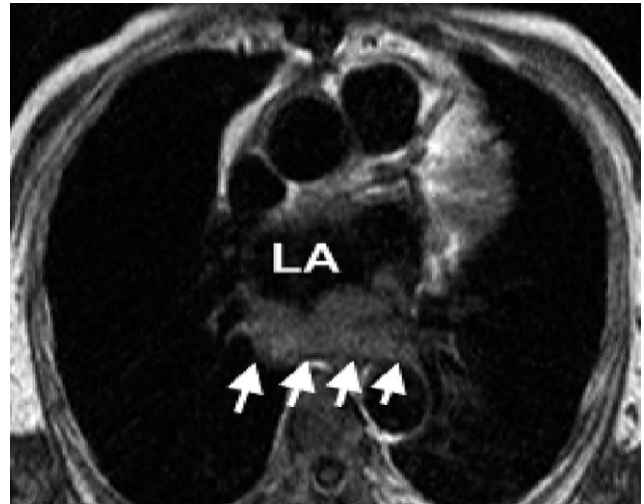


**FIG 2.** Leiomyosarcoma in a 38-year-old man with progressive dyspnea. Axial T1-weighted black-blood image showing a broad based infiltrative mass along the posterior wall of the left atrium (arrows). LA, left atrium.

### *Clinical Features and CMRI Appearances*

**Undifferentiated Sarcoma.** Undifferentiated sarcomas account for up to 25% of all primary cardiac tumors, although with improved immunohistochemistry techniques, their frequency may be declining as many previously undifferentiated tumor varieties may now be assigned to a named subtype. Most undifferentiated sarcomas arise within the left atrium and appear as a discrete infiltrative mass, usually along the posterior wall.<sup>16</sup> Signal intensity is usually isointense to myocardium on T1- and T2-weighted images with a heterogeneous enhancement pattern.<sup>17</sup>

**Leiomyosarcoma.** These lesions originate in the left atrium in 80% of cases, most often along its posterior wall with frequent infiltration into the pulmonary vein ostia.<sup>18</sup> Macroscopically, they are broad based with an often lobulated outline. Rarely, leiomyosarcoma can arise from the inferior vena cava and produce symptoms suggestive of right heart failure. CMRI findings are relatively nonspecific, with intermediate signal on T1-weighted and mildly increased signal intensity on T2-weighted black-blood images having been reported (Fig 2).<sup>19</sup>

**Fibrosarcoma.** These lesions originate within the left atrium in around 50% of cases, within either ventricle in 30% and from the pericardium in 20%.<sup>17</sup> CMRI findings are those of an infiltrative mass that typically has heterogeneous signal intensity on T1- and T2-weighted images.

**Liposarcoma.** These lesions do not have a predilection for any chamber and have also been reported to arise from the pericardium and valves. Some present with cardiac tamponade.<sup>20</sup> They rarely contain significant amounts of macroscopic fat to permit a confident diagnosis based on morphologic imaging characteristics and as such their CMRI features are nonspecific. Necrosis and hemorrhage may be prominent, which can give them heterogeneous high-signal intensity on T1-weighted images.<sup>21</sup>

**Osteosarcoma.** Primary cardiac osteosarcoma almost always originates within the left atrium and is usually a large bulky mass that invades into the pulmonary vein ostia and mitral valve. They may have osteoblastic, chondroblastic, or fibroblastic differentiation. Macroscopic calcification is frequently present, although calcification may not be readily apparent on CMRI as it appears as signal void on all sequences. As a result, they generally appear hypointense on T1-weighted sequences and hyperintense on T2-weighted sequences.<sup>22</sup> Multidetector computed tomography is better suited to the detection of calcific components highlighting the complementary role that multidetector computed tomography can offer for tumor assessment.

### Rhabdomyosarcoma

Embryonal rhabdomyosarcoma predominates in childhood and is the commonest primary pediatric cardiac tumor. Pleomorphic rhabdomyosarcoma is much less frequent and most commonly occurs in adulthood.<sup>10</sup> These tumors arise from the myocardium with no chamber predilection. There is a tendency toward multiple sites of origin and valvular involvement.

#### CMRI Features

CMRI appearances are those of a large infiltrative mass with irregular margins and a tendency to central necrosis and cavitation (Fig 3). They are isointense to myocardium on T1-weighted with central high signal on T2-weighted images.<sup>23</sup> The peripheral solid components usually display homogeneous delayed enhancement.<sup>24</sup>

### Primary Cardiac Lymphoma

Primary cardiac lymphoma is much more infrequent than secondary involvement and is defined as disease confined to the heart or pericardium with no evidence

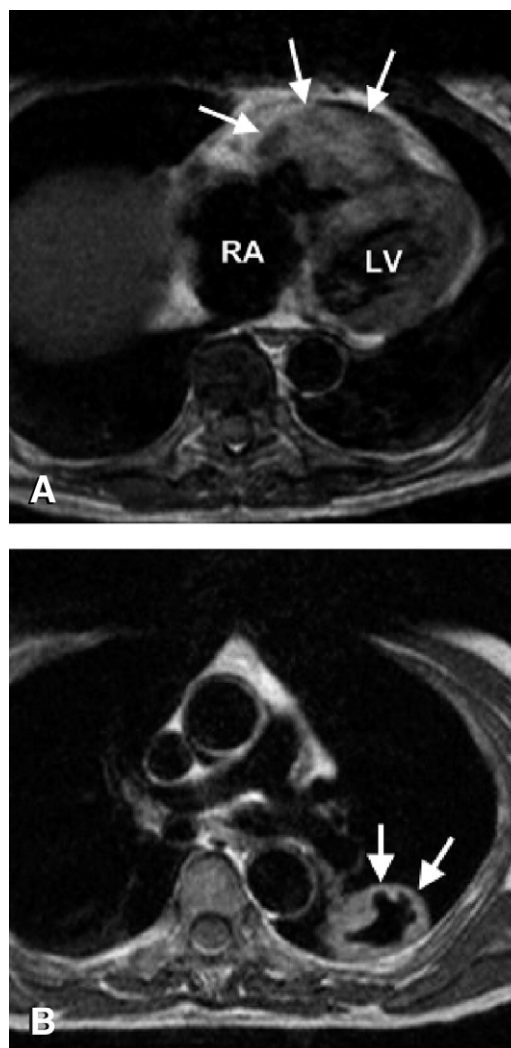


**FIG 3.** Rhabdomyosarcoma in a 71-year-old man with weight loss and worsening dyspnea. (A) Axial T1-weighted black-blood image showing a large isointense mass infiltrating through the right ventricular free wall (arrows). (B) Axial T1-weighted black-blood image at the level of the pulmonary artery bifurcation showing a large cavitating metastasis within the apical segment of the left lower lobe (arrows). RA, right atrium; LV, left ventricle.

of extracardiac disease.<sup>25</sup> It is exceedingly rare, representing 1.3% of primary cardiac tumors. The majority occurs in immunocompromised patients, is of B-cell origin, and follows an aggressive clinical course.<sup>26</sup> Mean age at presentation is 60 years with a slight male predominance. The right atrium is the commonest site of origin with frequent involvement of more than 1 chamber and pericardial invasion; a pericardial effusion may be the only finding. Unlike other cardiac tumors, treatment is primarily with anthracycline-based chemotherapy and monoclonal anti-CD20 antibody (rituximab).<sup>27</sup>



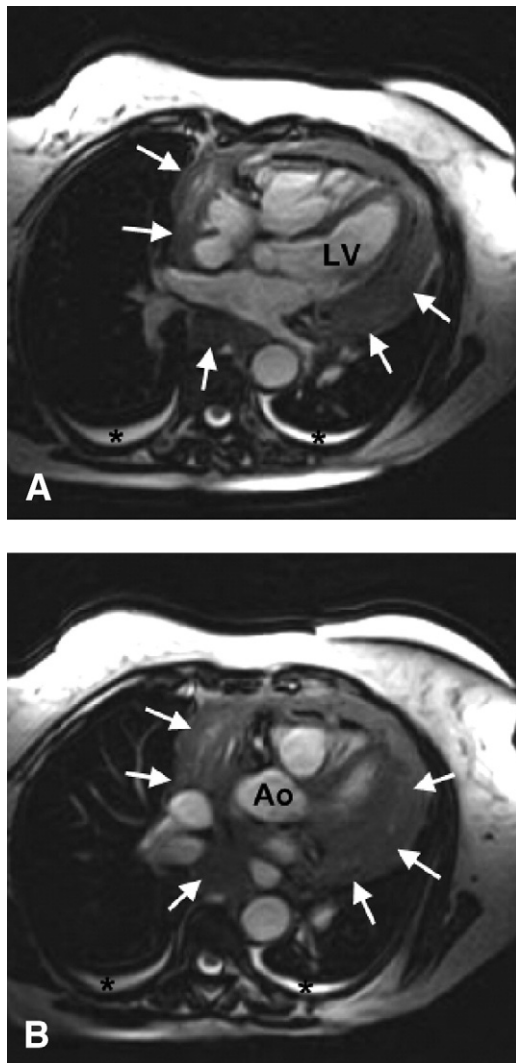


**FIG 4.** Primary cardiac lymphoma in a 42-year-old woman with no history of immunosuppression who presented with congestive cardiac failure. (A) Axial SSFP image at the level of the left atrium showing diffuse infiltration of the pericardial space by an intermediate signal intensity soft tissue mass (arrows). (B) Axial SSFP image at the level of the aortic root again showing diffuse infiltration of the pericardial space (arrows). LV, left ventricle; Ao, aorta.

### CMRI Features

Two main patterns are recognized on CMRI. The first (and most common) is that of multiple nodular masses infiltrating through the myocardium, with a predilection for the right ventricle. Tumor nodules are usually iso- or slightly hyperintense relative to normal myocardium and demonstrate heterogeneous enhancement.<sup>28</sup> The second pattern is that of diffuse pericardial infiltration in association with a hemorrhagic pericardial effusion (Fig 4).<sup>3</sup>

### Primary Pericardial Malignancy

Pericardial mesothelioma is a malignant neoplasm arising from the mesothelial cells of the pericardium and accounts for <1% of all thoracic mesotheliomas. Owing to the rarity of these tumors, a definitive causal relationship with asbestos exposure is yet to be established.<sup>29</sup> Mean age at presentation is 46 years and patients typically present with chest pain and signs of tamponade caused by pericardial infiltration and encasement. Significant myocardial infiltration is rare. As with pleural mesothelioma, treatment is predominantly palliative with few patients reported to survive more than 12 months following initial diagnosis.<sup>30</sup>

Pericardial synovial sarcoma is an extremely aggressive tumor composed of spindle and epithelioid cells that have similar clinical presentation and CMRI manifestations as cardiac angiosarcoma.

### CMRI Features

Pericardial mesothelioma appears as multiple enhancing and coalescing pericardial masses that obliterate the pericardial space. These tumors are isointense to myocardium on T1-weighted and heterogeneous on T2-weighted images.<sup>31</sup>

Pericardial synovial sarcoma appears as a heterogeneous lobulated mass, usually centered on the right atrial free wall and with extensive invasion into surrounding structures. First pass and delayed enhancement are usually avid (Fig 5).

### Cardiac Metastases

Cardiac metastases are 40-50 times more frequent than primary cardiac tumors but most remain clinically silent. The incidence ranges from 2.3% to 18.3%.<sup>32</sup> They generally appear late in the course of the primary disease and isolated cardiac involvement is rarely seen without dissemination to other organs. The pericardium is more frequently involved than myocardium and an associated malignant effusion may cause progressive breathlessness and signs of tamponade. Mechanisms of spread include direct extension, hematogenous or venous seeding, and retrograde flow via lymphatics.<sup>33</sup> Hematogenous seeding is the most common route of spread for tumors of bronchial and breast origin, followed by melanoma, lymphoma, and leukemia.<sup>3,34</sup> Transvenous extension to the right atrium via the inferior vena cava is a well-recognized complication of renal and hepatocellular carcinomas. Manage-

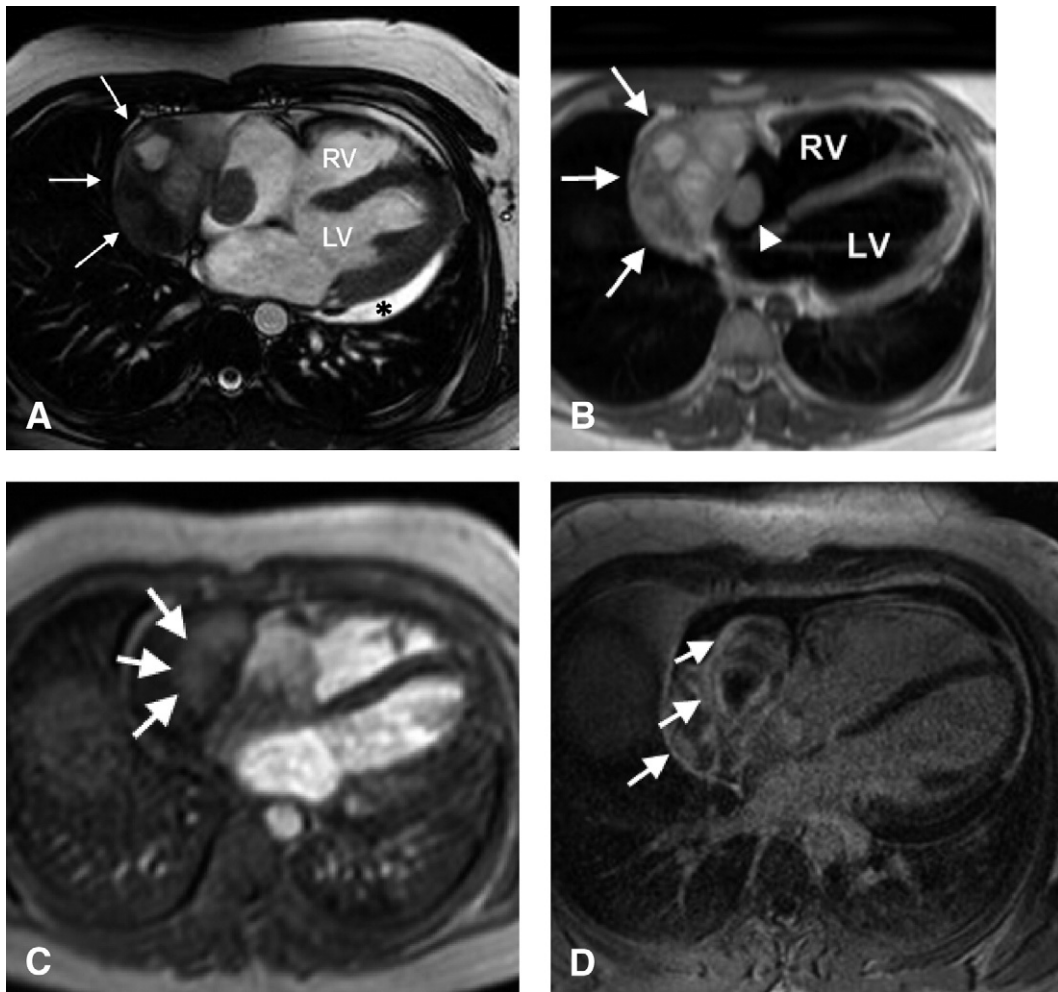


**FIG 5.** Primary synovial sarcoma in a 22-year-old man with chest pain. (A) Four-chamber SSFP image showing a large mixed signal intensity mass centered on the pericardial space overlying the right atrial free wall (arrows). A tongue of tumor is seen infiltrating into the right atrium and there is a small pericardial effusion (\*). (B) Axial T2-weighted black-blood image showing the mass to be of heterogeneously high T2 signal (arrows). Infiltration into the right atrium is again noted (arrowhead). (C) Axial image from dynamic gadolinium rest perfusion study showing intense central first-pass enhancement in keeping with a highly vascular lesion (arrows). (D) Axial T1-weighted delayed phase image obtained 10 minutes following gadolinium administration showing patchy enhancement in keeping with delayed contrast washout from tumor tissue (arrows). LV, left ventricle; RV, right ventricle.

ment is usually palliative for metastases from solid organ tumors with relief of tamponade by pericardiocentesis.

### CMRI Features

Imaging appearances of metastases are generally nonspecific and usually comprise enhancing masses or soft-tissue nodules. Melanoma has unique features owing to the T1 shortening properties of melanin and appears of high signal on T1-weighted images. A hemorrhagic pericardial effusion can be seen in association with metastases from any primary site (Fig 6).

### Tumor-Like Conditions

A variety of lesions can mimic benign and malignant cardiac tumors and should be recognized as such to avoid misdiagnosis and inappropriate management. Thrombus is by far the commonest tumor “mimic.”

### Intracardiac Thrombus

Thrombus is the major differential for any intracardiac mass, especially atrial myxoma, with which it shares a common site of origin. Thrombus has a particular predilection for the left atrial appendage, as this is a

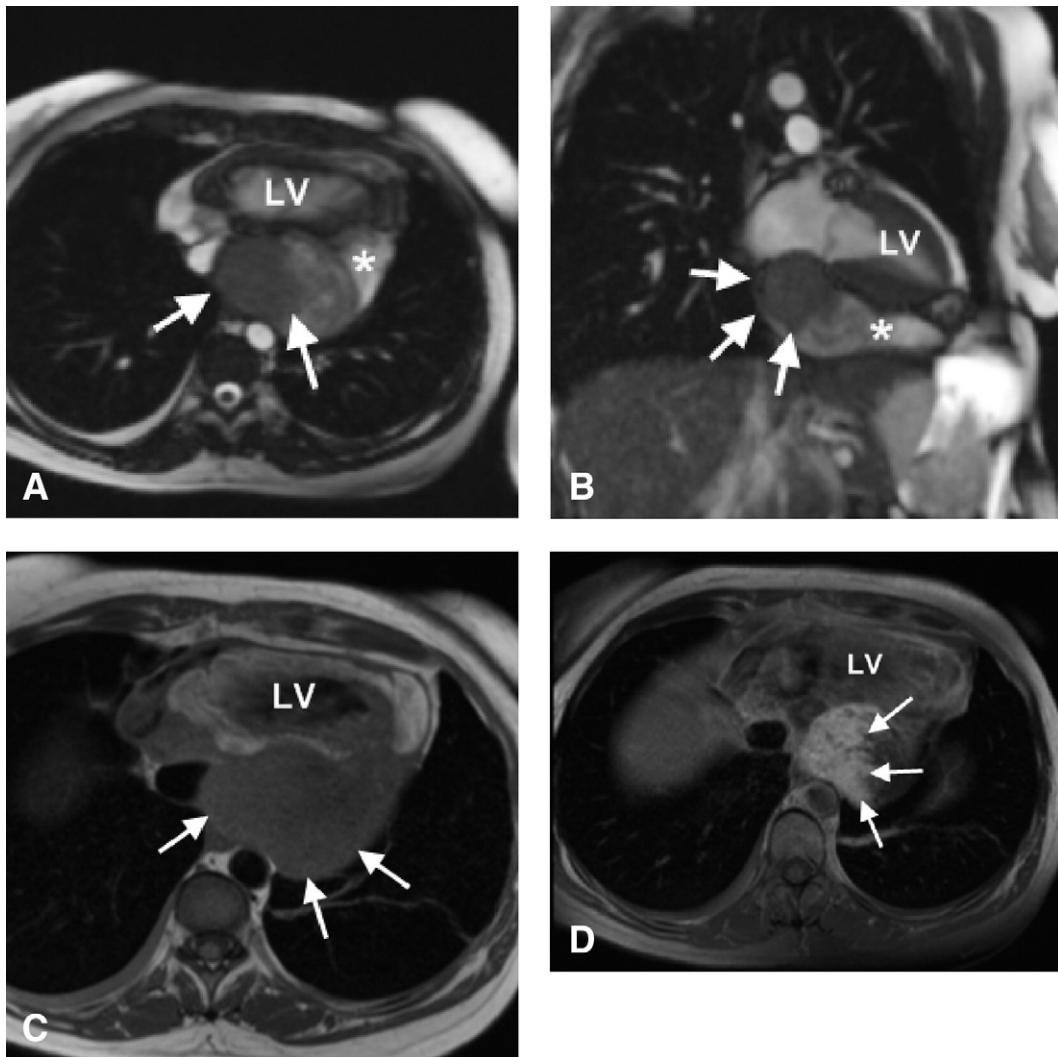


**FIG 6.** Pericardial metastasis in a 46-year-old woman with metastatic breast carcinoma who presented with chest pain and dyspnea. (A) Axial SSFP image showing a large heterogeneous signal intensity pericardial effusion (\*) with a solid component (arrows). (B) Two-chamber SSFP image showing the effusion (\*) and solid component (arrows), which is indenting the floor of the left atrium. (C) Axial T1-weighted black-blood image showing the solid component to be predominantly low signal intensity (arrows). (D) Axial T1-weighted delayed phase image obtained 10 minutes following gadolinium administration showing intense central enhancement of the solid component in keeping with delayed contrast washout from tumor tissue (arrows). LV, left ventricle.

site of slow blood flow, but myxoma may also arise in this location. Atrial fibrillation is a common predisposing factor for left atrial thrombus formation but may also occur secondary to myxoma. Other common locations for thrombus formation are the left ventricle, especially in association with aneurysm formation post myocardial infarction, and the right atrium, when there is a central venous catheter. Discriminating between thrombus and myxoma may not be possible with echocardiography or multidetector CT angiography, particularly with sessile or small myxomas that are often relatively immobile and may not show prolapse across the mitral valve orifice. Signal characteristics of myxoma and thrombus

overlap on CMRI, although a multisequence evaluation with both dynamic rest perfusion and delayed enhancement images is often sufficient to confidently discriminate between these 2 entities.

### CMRI Features

Signal intensity varies on T1- and T2-weighted images according to thrombus chronicity and contrast-enhanced sequences are therefore more useful. Thrombus appears as a nonenhancing low signal lesion on first pass perfusion and remains low signal on delayed enhancement images (Fig 7A-C).<sup>1</sup> In a study of 784 consecutive at-risk patients with systolic dysfunction,

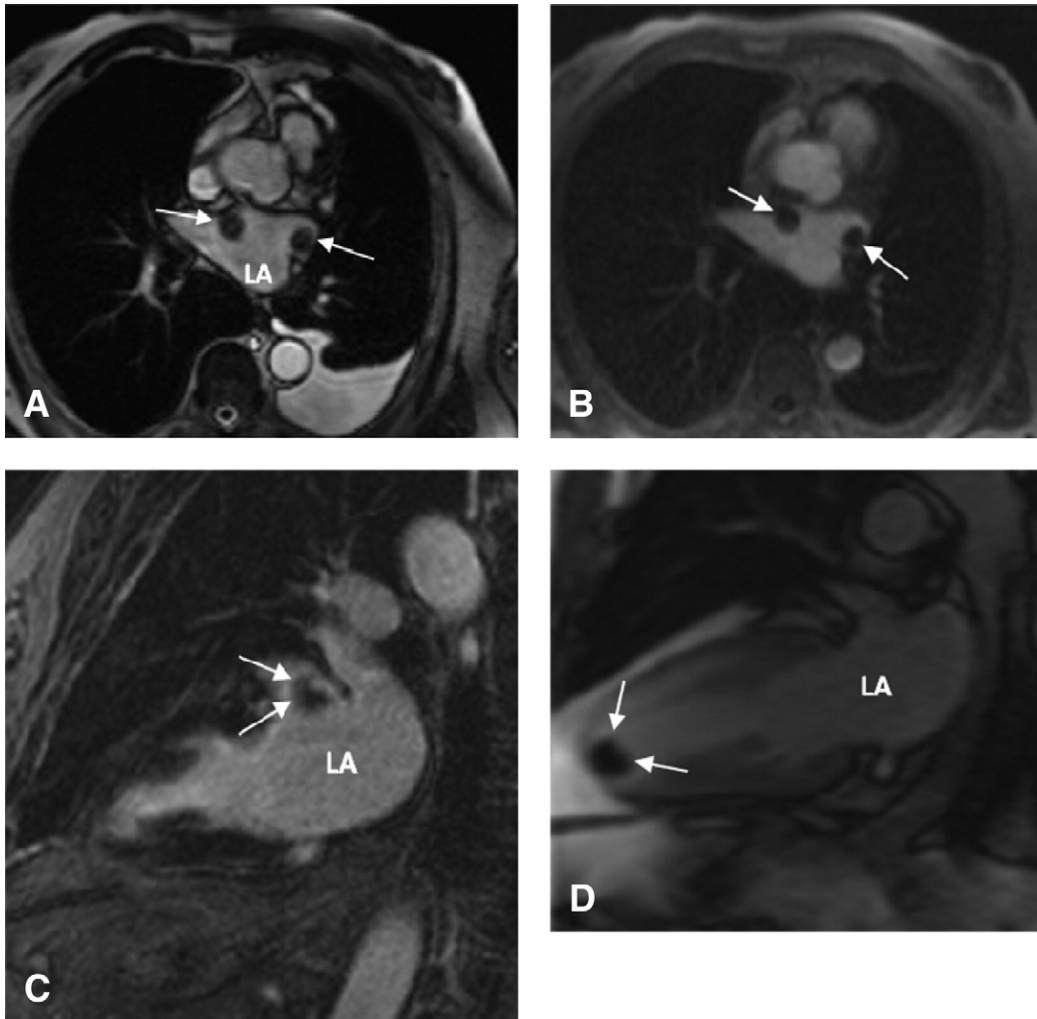


**FIG 7.** Left atrial thrombi (A-C) and left ventricular thrombus (D). (A) Axial SSFP image through the left atrium showing 2 well-circumscribed low signal lesions attached to the endocardium by a short stalk (arrows). Also note the presence of a left pleural effusion. The differential diagnosis was between multiple left atrial myxomas or thrombus. (B) Axial image from dynamic gadolinium rest perfusion study showing complete absence of first-pass enhancement in keeping with poorly vascularized lesions (arrows). (C) Two-chamber T1-weighted delayed phase image obtained 10 minutes following gadolinium administration showing complete absence of late enhancement within the most superior lesion (arrows). This combination of findings was most in favor of thrombus and these lesions resolved completely on follow-up imaging after a period of anticoagulation (not shown). (D) Two-chamber T1-weighted delayed phase image obtained 10 minutes following gadolinium administration and with selection of a long inversion time (600 ms). Thrombus within the left ventricle fails to invert (remains of low signal) compared with adjacent tissues (arrows). LA, left atrium.

delayed enhancement CMRI detected thrombus in 7% of patients compared with cine CMRI in 4.7%.<sup>35</sup> Selection of a long inversion time (>500 ms) for delayed enhancement imaging has also been shown to be very sensitive for detection of even small thrombi, which fail to invert (remain of low signal) compared with other tissues and in contrast to tumors (Fig. 7D).<sup>36</sup>

### Pericardial Cyst

Pericardial cysts are benign congenital lesions that arise from the pericardium but do not communicate

with the pericardial space. They have an incidence of 1 in 100,000 and are most commonly found at the right cardiophrenic angle, although they may occur anywhere in the mediastinum. They are simple unilocular lesions that contain water-based fluid without internal septa. Although usually asymptomatic, up to one third of patients may complain of symptoms, including chest pain, dyspnea, and persistent cough.<sup>37</sup>

### CMRI Features

Findings are those of a fluid intensity lesion (low T1- and high T2-signal) that does not enhance (Fig 8).



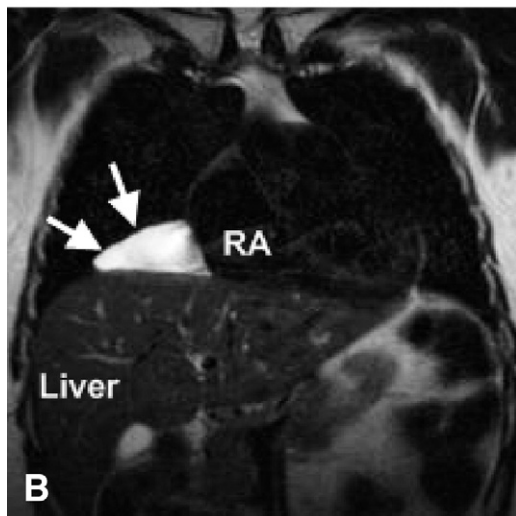


**FIG 8.** Pericardial cyst in an asymptomatic 50-year-old woman that was discovered on a thoracic CT examination with CMRI performed as a confirmatory study. (A) Coronal T1-weighted image showing a well-demarcated uniformly low-signal lesion at the right cardiophrenic angle (arrows). (B) Coronal T2-weighted image showing the lesion to be of uniformly high signal and without any internal septations (arrows). RA, Right atrium.

On occasion, a pericardial cyst may contain relatively proteinaceous fluid and thus can have high signal intensity on both T1-weighted and T2-weighted images.

### Bronchogenic Cyst

Bronchogenic cysts are well-circumscribed, thin-walled, fluid-filled structures that are thought to arise from the bronchial tree because of abnormal budding of the ventral foregut during the first trimester. Ap-



**FIG 9.** Bronchogenic cyst in a 43-year-old woman who presented with dysphagia. Coronal T2-weighted image showing a thin-walled uniformly high signal lesion within the middle mediastinum (arrows).

proximately two thirds are sited within the mediastinum, most often in a subcarinal or right paratracheal location.

### CMRI Features

A bronchogenic cyst appears as a well-circumscribed, usually rounded lesion that has variable signal intensity on T1-weighted images, dependent on the amount of proteinaceous content<sup>38</sup>; however, they are usually of uniformly high signal on T2-weighted images (Fig 9).

### Normal Anatomical Structures

The Crista terminalis is a vertically orientated fibromuscular ridge that runs along the posterior aspect of the right atrium and gives rise to the pectinate muscles, which fan out anteriorly. Its size and extent vary considerably among individuals and familiarity with this structure helps minimize misdiagnosis.<sup>39</sup> The moderator band extends across the right ventricle and contains the right bundle branch; it is a defining feature of the right ventricle and should not be mistaken for an intracardiac mass.

### Conclusions

Although there is considerable overlap in both the presenting symptoms and the imaging appearances of

cardiac and pericardial malignancy, features, such as age at presentation (childhood or adulthood), site of involvement (right vs left side of the heart), size, signs of invasive behavior, presence of concurrent effusions (pericardial or pleural), and tissue characteristics, all help to narrow the differential diagnosis. CMRI is now recognized as the reference noninvasive imaging technique for assessment and characterization of a suspected cardiac or juxta-cardiac mass. The multiplanar assessment of anatomy, tissue composition, and functional impact afforded by CMRI allows for early differentiation between a nonneoplastic mass and a tumor mass, be it benign or malignant. Benign primary cardiac tumors will often be referred for prompt surgical resection, which is generally associated with low morbidity and favorable long-term outcomes. Malignant primary cardiac tumors by contrast carry a dismal prognosis even with aggressive surgical debulking and adjuvant chemotherapy. Cardiac metastases generally occur late in the course of disseminated malignancy and many not cause significant clinical effects except when associated with a large pericardial effusion. CMRI is increasingly used for investigation of a suspected mass and the imaging specialist should be familiar with protocol design, a systematic approach to assessment and key findings across the spectrum of benign and malignant lesions.

## REFERENCES

1. Sparrow PJ, Kurian JB, Jones TR, et al. MR imaging of cardiac tumors. *Radiographics* 2005;25:1255-76.
2. Grizzard JD, Ang GB. Magnetic resonance imaging of pericardial disease and cardiac masses. *Magn Reson Imaging Clin N Am* 2007;15:579-7.
3. Chiles C, Woodard PK, Gutierrez FR, et al. Metastatic involvement of the heart and pericardium: CT and MR imaging. *Radiographics* 2001;21:439-49.
4. Donsbeck AV, Ranchere D, Coindre JM, et al. Primary cardiac sarcomas: An immunohistochemical and grading study with long-term follow-up of 24 cases. *Histopathology* 1999;34:295-304.
5. Neragi-Miandoab S, Kim J, Vlahakes GJ. Malignant tumours of the heart: A review of tumour type, diagnosis and therapy. *Clin Oncol* 2007;19:748-56.
6. Liu Y, Ghesani NV, Zuckier LS. Physiology and pathophysiology of incidental findings detected on FDG-PET scintigraphy. *Semin Nucl Med* 2010;40:294-315.
7. Higashiyama S, Kawabe J, Hayashi T, et al. Effectiveness of preoperative PET examination of huge angiosarcoma of the heart. *Clin Nucl Med* 2009;34:99-102.
8. Hoffmann U, Globits S, Schima W, et al. Usefulness of magnetic resonance imaging of cardiac and paracardiac masses. *Am J Cardiol* 2003;92:890-5.
9. Lam KY, Dickens P, Chan AC. Tumors of the heart. A 20-year experience with a review of 12,485 consecutive autopsies. *Arch Pathol Lab Med* 1993;117:1027-31.
10. Burke A, Virmani R. Tumors of the heart and great vessels. In: *Atlas of Tumor Pathology*. Washington, D.C.: Armed Forces Institute of Pathology, 1996.
11. Best AK, Dobson RL, Ahmad AR. Best cases from the AFIP: Cardiac angiosarcoma. *Radiographics* 2003;23:S141-5.
12. Janigan DT, Husain A, Robinson NA. Cardiac angiosarcomas: A review and a case report. *Cancer* 1986;57:852-9.
13. Pigott C, Welker M, Khosla P, et al. Improved outcome with multimodality therapy in primary cardiac angiosarcoma. *Nat Clin Pract Oncol* 2008;5:112-5.
14. Deetjen AG, Conradi G, Mollmann S, et al. Cardiac angiosarcoma diagnosed and characterized by cardiac magnetic resonance imaging. *Cardiol Rev* 2006;14:101-3.
15. Yahata S, Endo T, Honma H, et al. Sunray appearance on enhanced magnetic resonance image of cardiac angiosarcoma with pericardial obliteration. *Am Heart J* 1994;127:468-71.
16. Itoh K, Matsumura T, Egawa Y. Primary mitral valve sarcoma in infancy. *Pediatr Cardiol* 1998;19:174-7.
17. Araoz PA, Eklund HE, Welch TJ, et al. CT and MRI of primary cardiac malignancies. *Radiographics* 1999;19:1421-34.
18. Clarke NR, Mohiaddin RH, Westaby S, et al. Multifocal cardiac leiomyosarcoma: Diagnosis and surveillance by transoesophageal echocardiography and contrast-enhanced cardiovascular magnetic resonance. *Postgrad Med J* 2002;78:492-3.
19. Lo FL, Chou YH, Tiu CM, et al. Primary cardiac leiomyosarcoma: Imaging with 2-D echocardiography, electron beam CT and 1.5-Tesla MR. *Eur J Radiol* 1998;27:72-6.
20. Kitamura A, Ozaki N, Mukohara N, et al. Primary cardiac liposarcoma causing cardiac tamponade: Report of a case. *Surg Today* 2007;37:974-6 [Epub October 25, 2007].
21. Schrem SS, Colvin SB, Weinreb JC, et al. Metastatic cardiac liposarcoma: Diagnosis by transesophageal echocardiography and magnetic resonance imaging. *J Am Soc Echocardiogr* 1990;3:149-53.
22. Yamagishi M, Yamada N, Kuribayashi S. Images in cardiology: Magnetic resonance imaging of cardiac osteosarcoma. *Heart* 2001;85:311.
23. Gilkeson RC, Chiles C. MR evaluation of cardiac and pericardial malignancy. *Magn Reson Imaging Clin N Am* 2003;1:173-86.
24. Villacampa VM, Villarreal M, Ros LH, et al. Cardiac rhabdomyosarcoma: Diagnosis by MR imaging. *Eur Radiol* 1999;9:634-7.
25. Burke A. Primary malignant cardiac tumors. *Semin Diagn Pathol* 2008;25:39-46.
26. Ceresoli GL, Ferreri AJ, Bucci E, et al. Primary cardiac lymphoma in immunocompetent patients. *Cancer* 1997;80:1497-506.
27. Burke A, Jeudy J Jr, Virmani R. Cardiac tumours: An update. *Heart* 2008;94:117-23.
28. Ryu SJ, Choi BW, Choe KO. CT and MR findings of primary cardiac lymphoma: Report upon 2 cases and review. *Yonsei Med J* 2001;42:451-6.
29. Butany J, Nair V, Naseemuddin A, et al. Cardiac tumours: Diagnosis and management. *Lancet Oncol* 2005;6:219-28.

30. Kainuma S, Masai T, Yamauchi T, et al. Primary malignant pericardial mesothelioma presenting as pericardial constriction. *Ann Thorac Cardiovasc Surg* 2008;14:396-8.
31. Ohnishi J, Shiotani H, Ueno H, et al. Primary pericardial mesothelioma demonstrated by magnetic resonance imaging. *Jpn Circ J* 1996;60:898-900.
32. Bussani R, De-Giorgio F, Abbate A, et al. Cardiac metastases. *J Clin Pathol* 2007;60:27-34.
33. Chiles C, Woodard PK, Gutierrez FR, et al. Metastatic involvement of the heart and pericardium: CT and MR imaging. *Radiographics* 2001;21:439-49.
34. Hancock EW. Neoplastic pericardial disease. *Cardiol Clin* 1990;8:673-82.
35. Weinsaft JW, Kim HW, Shah DJ, et al. Detection of left ventricular thrombus by delayed-enhancement cardiovascular magnetic resonance prevalence and markers in patients with systolic dysfunction. *J Am Coll Cardiol* 2008;52:148-57.
36. Scrichai MB, Junor C, Rodriguez LL, et al. Clinical, imaging and pathological characteristics of left ventricular thrombus: A comparison of contrast-enhanced magnetic resonance imaging, transthoracic echocardiography, and transesophageal echocardiography with surgical or pathological validation. *Am Heart J* 2006;152:75-84.
37. Feigin DS, Femoglio JJ, McAllister HA, et al. Pericardial cysts: A radiologic-pathologic correlation and review. *Diagn Radiol* 1977;125:15-20.
38. Nakata H, Egashira K, Watanabe H, et al. MRI of bronchogenic cysts. *J Comput Assist Tomogr* 1993;17:267-70.
39. Broderick LS, Brooks GN, Kuhlman JE. Anatomic pitfalls of the heart and pericardium. *Radiographics* 2005;25:441-53.